

---

# NETBURST: EVENT-CENTRIC FORECASTING OF BURSTY, INTERMITTENT TIME SERIES

Satyandra Guthula<sup>1</sup>Ashish Kundu<sup>2</sup>Jaber Daneshamooz<sup>1</sup>Walter Willinger<sup>3</sup>Charles Fleming<sup>2</sup>Arpit Gupta<sup>1</sup><sup>1</sup>University of California, Santa Barbara<sup>2</sup>Cisco Research<sup>3</sup>NIKSUN Inc.

## ABSTRACT

Forecasting on widely used benchmark time series data (e.g., ETT, Electricity, Taxi, and Exchange Rate, etc.) has favored smooth, seasonal series, but *network telemetry time series*—traffic measurements at service, IP, or subnet granularity—are instead *highly bursty and intermittent*, with heavy-tailed bursts and highly variable inactive periods. These properties place the latter in the statistical regimes made famous and popularized more than 20 years ago by B. Mandelbrot. Yet forecasting such time series with modern-day AI architectures remains underexplored. We introduce NETBURST, an event-centric framework that reformulates forecasting as predicting *when* bursts occur and *how large* they are, using quantile-based codebooks and dual autoregressors. Across large-scale sets of production network telemetry time series and compared to strong baselines, such as Chronos, NETBURST reduces Mean Average Scaled Error (MASE) by 13–605× on service-level time series while preserving burstiness and producing embeddings that cluster 5× more cleanly than Chronos. In effect, our work highlights the benefits that modern AI can reap from leveraging Mandelbrot’s pioneering studies for forecasting in bursty, intermittent, and heavy-tailed regimes, where its operational value for high-stakes decision making is of paramount interest.

## 1 INTRODUCTION

Time-series forecasting (Lim & Zohren, 2021) underpins critical decisions across domains, from finance and economics to climate science and healthcare. Recent progress has been propelled by benchmark datasets such as ETT (Zhou et al., 2021), Electricity (Trindade, 2015), Taxi (Misar, 2022), and Exchange Rate (Federal Reserve, 2022). These datasets share a common structure: they are smooth and exhibit moderate fluctuations around a seasonally varying average, with tightly bounded variance and pronounced periodicities. Forecasters trained on such data implicitly learn the “language” of continuity and regularity—and thrive within it.

**Requirements for network telemetry.** Network telemetry time series speak a very different language. Derived from measurements of traffic and devices (e.g., routers, servers, or clients), they track demand and performance at multiple granularities: *service* (applications and protocols), *IP* (individual hosts), and *subnet* (aggregated groups of hosts). Each granularity matters operationally—service forecasts guide quality assessment, IP forecasts power anomaly detection, and subnet forecasts support traffic engineering. Yet across all levels, telemetry data is *highly bursty and intermittent*: burst sizes, durations, and lull periods all follow heavy-tailed laws. As emphasized in (Wierman, 2023; Willinger et al., 2005), “heavy tails are more normal than the Normal”—extreme events are not rare exceptions but defining features of these distributions. This places network telemetry in the statistical regimes that were originally shown to be of practical relevance by Mandelbrot and include fractals, self-similar scaling,  $1/f$  noise, and long-range dependence—phenomena observed not only in networking but also in finance, weather, and economics datasets (Mandelbrot, 1982; 1997; Mason, 2016).

**Limitations of existing forecasters.** Today’s state-of-the-art models collapse under these requirements. Transformer-based forecasters such as Chronos (Ansari et al., 2024) and Lag-Llama (Rasul et al., 2023a) conflate irregular burst timing with extreme magnitudes, smoothing away the very

Dataset	Chronos	DeepAR	Lag-Llama	N-BEATS
Electricity (15m)	0.2263	0.4080	0.2036	0.4243
Taxi (30m)	0.5964	0.7258	0.6213	0.5851
ETT-M2 (hourly)	0.1025	0.1213	0.150	1.0034
Weather (daily)	0.3564	0.5759	0.4154	1.0455
Exchange Rate (daily)	0.0253	0.0567	0.0432	0.0581
Pinot (service, 100ms)	18.1282	1.0019	2.2851	46.35
Pinot (IP, 1s)	782.3511	2.2039	2.6170	86.47
Pinot (subnet, 1s)	1640.4	1.9807	1.9751	95.53
MAWI (service, 100ms)	2.1782	0.9994	1.0161	35.5556
MAWI (IP, 1s)	1629.3	8.8251	34.5436	44.9187
MAWI (subnet, 1s)	13.4595	5.1334	13.7958	98.6089

Table 1: SOTA performance (MASE) on existing benchmarks vs. network telemetry.

events operators care about. Continuous-time point-process models capture sparsity but fail to handle heavy-tailed magnitudes and long-range dependence. Even advanced tokenizers, like Chronos’s uniform binning, waste resolution on dense mid-ranges while erasing fidelity in the tails. The result is forecasting errors up to three orders of magnitude larger on production telemetry datasets such as PINOT (Beltiukov et al., 2023) and MAWI (Maw, 2025) (Table 1).

**Our proposal.** This gap motivates a new paradigm. While the statistical properties of heavy-tailed, intermittent time series are well documented (Nair et al., 2013; Resnick, 2007; Beran, 1994), how to forecast them with modern architectures remains scientifically underexplored (Hasan et al., 2023). In essence, by presenting NETBURST, an event-centric framework that reframes forecasting as disentangling *when* bursts occur and *how large* they are, our work is an instance of *Mandelbrot meets AI*. By combining distribution-aware quantile tokenization with dual autoregressive models, NETBURST allocates capacity to rare, high-impact events while preserving scalability. In doing so, we adapt foundation-style forecasters from the smooth, seasonal regimes of past benchmarks to the bursty, intermittent, heavy-tailed domains where operational impact lies.

### Contributions.

- We introduce NETBURST, an event-centric forecasting framework that separates inter-burst gaps (timing) from burst intensities (magnitude), tokenized via quantile-based codebooks and modeled with dual autoregressors.
- We demonstrate substantial improvements over state-of-the-art forecasters on large-scale network telemetry datasets (PINOT, MAWI) across service, IP, and subnet granularities. On service-level traces, NETBURST reduces MASE to 0.0766 (PINOT) and 0.0762 (MAWI), yielding improvements ranging from 13–605 $\times$  compared to existing SOTA forecasters.
- We show that NETBURST preserves burstiness: large pointwise error reductions are achieved without distorting distributional fidelity. Across subnet-level traces, NETBURST improves Wasserstein distance (WD) (Panaretos & Zemel, 2019) by roughly 2–3 $\times$  relative to strong sequence forecasters, while on service-level traces, its WD remains competitive with the best baselines.
- We evaluate embedding quality, showing that NETBURST improves clustering quality: silhouette scores (Shahapure & Nicholas, 2020) improve by more than 5 $\times$  at small  $k$  compared to baselines.

## 2 BACKGROUND AND MOTIVATION

**Network telemetry data is highly bursty and intermittent.** Recent progress in time-series forecasting has been driven by benchmarks such as ETT (Zhou et al., 2021), Electricity (Trindade, 2015), Taxi (Misar, 2022), and Exchange Rate (Federal Reserve, 2022). These datasets capture discrete-time temporal fluctuations around a mean and seasonal dynamics (Box et al., 1978), and models that perform well on them often rely on implicit assumptions of smooth and cyclic or periodic behavior. For example, the ETT dataset records electricity transformer temperatures and loads at fixed intervals, exhibiting clear daily and weekly cycles. Similarly, the New York City Taxi dataset tracks the

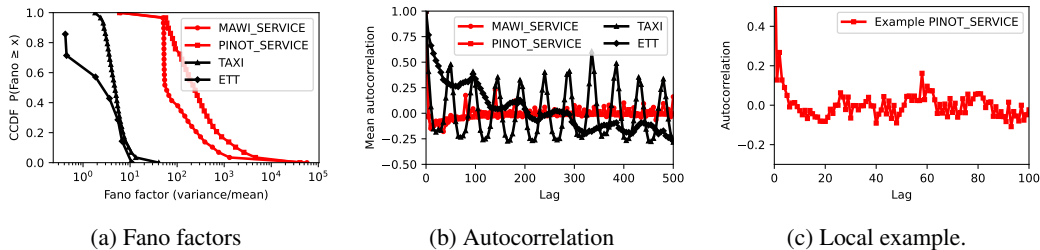


Figure 1: Current forecasting benchmarks (ETT and Taxi) vs. network telemetry data (more bursty service time series): (a) shows benchmarks are confined to narrow ranges, while network telemetry exhibits extreme variability. (b) reveals strong periodicity in benchmarks but flat autocorrelation structure in telemetry. (c) shows telemetry has only localized, phase-misaligned micro-patterns that cancel when aggregated.

number of rides over time, showing pronounced diurnal and weekly patterns. These benchmarks are characterized by bounded variance, non-bursty activity, and pronounced periodic patterns.

However, these properties fail to capture the statistical features of real-world *network telemetry time series*—measurements collected from production network traffic or devices (e.g., routers, end-hosts) to monitor performance, reliability, and security. Network telemetry metrics (e.g., packet or byte counts) are often aggregated at different spatial granularities—*service* (applications and protocols), *IP* (individual hosts), and *subnet* (groups of hosts)—to provide a holistic view of network state. Forecasting at each granularity serves distinct operational goals: service-level forecasts inform quality assessment and classification, IP-level forecasts support anomaly detection and intrusion monitoring, and subnet-level forecasts guide traffic engineering and capacity planning Guok et al. (2025).

In contrast to existing benchmarks, network telemetry time series are *highly bursty and intermittent*, with burst sizes, burst durations, and lull periods all typically following heavy-tailed distributions (Nair et al., 2013). Most activity is modest, but rare events can be orders of magnitude larger than the mean and dominate both the magnitude and variability of the traffic. Figure 1 quantifies these statistical differences<sup>1</sup>. Figure 1a shows the CCDF of Fano factors (variance-to-mean ratios) Fano (1947) across datasets: while benchmark series concentrate within narrow bounds, telemetry time series exhibit heavy-tailed behavior, reflecting entities whose traffic is dominated by rare, extreme bursts. Figure 1b depicts empirical autocorrelation functions Box et al. (2015) across datasets. While benchmarks exhibit clear periodic patterns indicative of seasonal cycles, telemetry traces show no signs of periodic behavior, and the autocorrelations remain flat at scale. For example, when zooming-in on the initial portion of the empirical autocorrelation function for one of the telemetry time series (Pinot-service), Figure 1c shows localized micro-patterns, which are phase-misaligned and cancel when aggregated.

Table 1 highlights the collapse of state-of-the-art forecasters when applied to bursty, intermittent telemetry. Models tuned to smooth, seasonal datasets fail by one to three orders of magnitude on PINOT and MAWI precisely because they smooth over rare bursts or default to trivial predictions. DeepAR (Salinas et al., 2020) minimizes loss in sparse regimes by predicting all zeros, while N-BEATS (Oreshkin et al., 2020), designed around periodic templates, extracts no meaningful structure. Even models like Chronos (Ansari et al., 2024) and Lag-Llama (Rasul et al., 2023a), which claim to succeed without time-series-specific biases, implicitly assume continuity and bounded variance: Chronos’s “agnostic to time” design works on smooth benchmarks but erases timing and tail fidelity in telemetry, and its reported zero-shot generalization holds only for non-bursty regimes. The implication is clear: forecasting telemetry requires elevating bursts to first-class modeling units, rather than treating the series as continuous fluctuations around a seasonal mean.

**Sparsity and entanglement break sequence models.** Sparse time series exacerbate this challenge. Bursts are rare and widely separated, so capturing them requires long context windows. However, naïvely extending sequence length is wasteful: most tokens correspond to idle or noisy intervals.

<sup>1</sup>We observe similar trends for other benchmarks and granularities for telemetry data

---

Models either dilute bursts among zeros or learn shortcuts, such as predicting zero everywhere. This explains the misleadingly low errors of DeepAR on some sparse series—it minimizes loss by ignoring rare events entirely. Even when bursts are predicted, monolithic models conflate *when* they occur and *how large* they are. These two distributions—inter-burst gap (IBG) and burst intensity (BI)—have distinct statistical behavior. Sequence models that treat them jointly allocate capacity inefficiently, leading to unstable forecasts. As our Oracle analyses in Section 4.3 confirm, IBG dominates error on sparse service traces, while BI dominates on denser IP/subnet traces. This motivates disentangling timing from magnitude, using separate prediction streams with light coupling.

**Uniform binning under-represents tails.** Tokenized foundation models such as Chronos (Ansari et al., 2024) introduce discretization, but use uniform bins. This allocates resolution evenly across the value range, oversampling dense low-magnitude fluctuations and undersampling rare, high-magnitude bursts. On existing datasets, this is adequate, but in telemetry, it systematically erases the very events that dominate tail error. Table 1 illustrates this directly: despite pretraining, Chronos collapses on network telemetry data. These results call for distribution-aware codebooks that allocate bins according to probability mass, preserving tail fidelity.

**Embeddings collapse under baselines.** Forecasting performance is only part of the story. Operators often need to cluster entities, detect anomalies, or transfer models across contexts. Embeddings from existing models collapse in these regimes: they show high anisotropy and poor clustering quality, dominated by trivial small fluctuations rather than bursts. This undermines downstream tasks as much as forecasting. We show in Section 4.5 that event-centric embeddings—derived from IBG and BI token streams—yield richer and more isotropic representations.

**Beyond networking telemetry.** This bursty, intermittent behavior is not unique to networking; it reflects statistical phenomena extensively studied by Mandelbrot, who introduced concepts such as *fractals*, *self-similar scaling*, *1/f noise*, and *long-range dependence* to describe heavy-tailed time series in domains like telecommunications, finance, economics, and weather (Mandelbrot, 1982; 1997; Leland et al., 2002; Verma et al., 2025). Existing state-of-the-art forecasters are likely to encounter similar challenges in these settings. Although the statistical properties of such processes are well established, how to forecast them effectively with modern architectures such as transformers remains scientifically underexplored despite their operational importance.

### 3 EVENT-CENTRIC FORECASTING WITH NETBURST

**Overview: From sequences to events.** Forecasting network telemetry time series with conventional sequence models fails for several reasons established in Section 2: sparsity caused by bursty and intermittent behavior makes long contexts inefficient, timing- and magnitude-related aspects are entangled in ways that destabilize predictions, uniform binning ignores or discounts heavy-tailed extremes, and learned embeddings collapse under skewed activity.

To address these issues, we adopt a different guiding principle: reframe forecasting as an *event prediction problem* rather than a direct sequence-value regression task. Instead of predicting raw time series values (i.e., byte counts) at every step, we represent telemetry time series as a sequence of bursts, each defined by **when** it occurs and **how large** it is. This decomposition parallels the structure of a marked Hawkes process Hawkes (1971): inter-burst gaps (IBG) capture event timings, while burst intensities (BI) serve as continuous marks. However, unlike traditional Hawkes models (Zuo et al., 2020; Meng et al., 2024), our formulation remains scalable, token-based, and able to accommodate heavy-tailed magnitudes.

More precisely, our pipeline proceeds in four steps as shown in Figure 2. (i) *Eventization*: convert time series into IBG and BI streams, compressing idle periods while preserving burst statistics. (ii) *Quantile tokenization*: discretize each stream with distribution-aware codebooks that allocate resolution to rare, extreme bursts. (iii) *Dual autoregressive models*: predict IBG and BI independently with autoregressive transformers, disentangling timing from magnitude while preserving local dependence. (iv) *Reconstruction*: recombine predicted events into byte-rate forecasts that retain both timing and magnitude fidelity. This event-centric design operationalizes the statistical properties documented in Section 2 into a forecasting framework that directly addresses the failure modes of existing models while preserving the self-exciting burst dynamics inherent to network telemetry data.

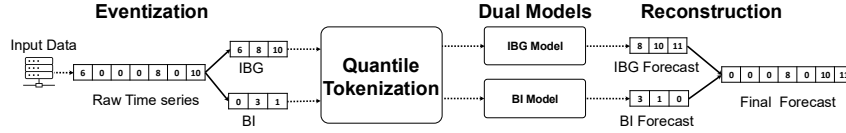


Figure 2: NETBURST pipeline. Raw telemetry series are eventized into inter-burst gaps (IBG) and burst intensities (BI), discretized with quantile-based tokenizers, and modeled with separate autoregressive forecasters. The two streams are then recombined during reconstruction to produce byte-count forecasts that preserve sparsity and burst fidelity.

**Eventization: Separating timing from magnitude.** Directly modeling network telemetry time series is problematic: most windows contain little or no traffic, so long contexts waste capacity on zeros; and when bursts do occur, their *timing* and *magnitude* are entangled in ways that destabilize forecasts (see Section 2). To address this problem, we reformulate forecasting as an event sequence prediction task.

Specifically, given a series  $s_{1:T}$ , we fix an activity threshold  $T_{\text{act}}$  and declare a *burst* whenever consecutive windows exceed this threshold. Each burst  $[\tau_k, \rho_k]$  is summarized by two values: the *inter-burst gap*  $\text{IBG}_k = \tau_k - \tau_{k-1}$  (with  $\text{IBG}_1 = \tau_1$ ) capturing **when** the burst occurs, and the *burst intensity*  $\text{BI}_k = \sum_{t=\tau_k}^{\rho_k} s_t$  capturing **how large** the burst is.

This transformation collapses long idle stretches into a single large IBG and replaces each burst with a compact BI mark. The resulting eventized sequence is far shorter and less noisy than the raw time series, yet it retains exactly the information needed for forecasting: the distribution of gaps between bursts and the heavy-tailed distribution of burst sizes. By disentangling timing from magnitude, eventization not only reduces wasted context but also makes the self-exciting burst structure of network traffic explicit.

**Quantile Tokenization: Preserving Heavy Tails.** Uniform binning, as used in Chronos (Ansari et al., 2024), wastes resolution on dense mid-range values and severely under-represents the rare, extreme events that dominate heavy-tailed telemetry time series. As mentioned in Section 2, this mismatch leads baselines to smooth away precisely the bursts that matter most in practice.

To address this issue, NETBURST replaces uniform binning with *quantile-based codebooks*. Instead of dividing the value range evenly, we discretize each stream so that every token corresponds to an equal fraction of probability mass. Specifically, we construct global quantile codebooks  $Q^{\text{IBG}}, Q^{\text{BI}}$  such that each bin holds approximately equal mass on the training data.

At training time, each observed inter-burst gap (IBG) or burst intensity (BI) is mapped to a token index  $z_k^{\text{IBG}}, z_k^{\text{BI}} \in \{1, \dots, B\}$  according to its quantile bin. Forecasting then reduces to next-token prediction, and reconstruction replaces each token with its bin centroid  $\hat{Q}^{\text{IBG}}, \hat{Q}^{\text{BI}}$ . This way, we preserve the shape of heavy tails, stabilize learning, and enable NETBURST to represent rare but operationally critical events as faithfully as routine fluctuations.

**Dual Models: Forecasting timing and magnitude separately.** Even after eventization and quantile tokenization, forecasting remains unstable if timing and magnitude are forced through a single prediction head. Models such as DeepAR or Lag-Llama conflate these dimensions, causing errors in one component to cascade into the other.

To address this problem, NETBURST employs two autoregressive transformer models: one for inter-burst gaps (IBG) and one for burst intensities (BI). Each model predicts its quantile-tokenized stream independently, i.e.,  $f_\theta : (z_{<k}^{\text{IBG}}) \mapsto p_\theta(z_k^{\text{IBG}} | z_{<k}^{\text{IBG}})$  and  $g_\psi : (z_{<k}^{\text{BI}}) \mapsto p_\psi(z_k^{\text{BI}} | z_{<k}^{\text{BI}})$ .

*Training.* Each model minimizes next-token cross-entropy with teacher forcing:  $\mathcal{L}_{\text{IBG}} = \sum_k -\log p_\theta(z_k^{\text{IBG}} | z_{<k}^{\text{IBG}})$  and  $\mathcal{L}_{\text{BI}} = \sum_k -\log p_\psi(z_k^{\text{BI}} | z_{<k}^{\text{BI}})$ .

*Inference.* During decoding, IBG and BI tokens are generated autoregressively,  $\hat{z}_k^{\text{IBG}} \sim p_\theta(\cdot | \hat{z}_{<k}^{\text{IBG}})$  and  $\hat{z}_k^{\text{BI}} \sim p_\psi(\cdot | \hat{z}_{<k}^{\text{BI}})$ , then mapped back to numeric values through their quantile codebooks  $Q^{\text{IBG}}$  and  $Q^{\text{BI}}$ . This separation stabilizes learning, avoids error entanglement, and allocates modeling capacity where it is most needed.

**Reconstruction: From events back to series.** The final step is to transform predicted event streams into a standard byte-count series usable by networking tasks. Predicted IBGs are accumulated into

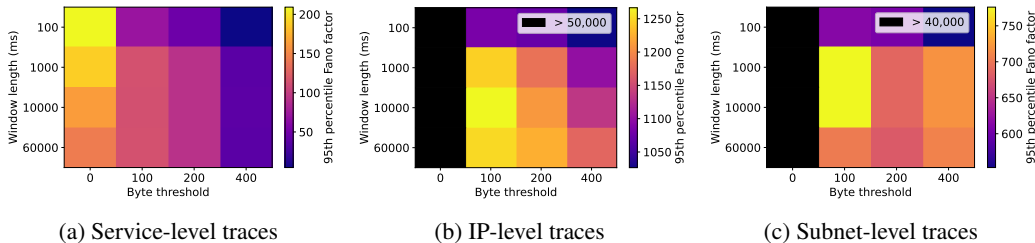


Figure 3: Fano Factor of the 95th-percentile service, IP, and subnet series under varying thresholds and window sizes. Smaller windows increase variance and sparsity, while larger windows reduce burst detail. This motivates the choice of 100 ms and 1 s windows for service- and IP/subnet-level evaluation, respectively.

absolute event times,  $\hat{\tau}_k = \hat{\tau}_{k-1} + \text{IB}\hat{G}_k$ , and paired with their predicted burst intensities,  $\hat{\text{BI}}_k$ . By default, we allocate each predicted burst entirely to its starting window (“spike placement”), though richer intra-burst kernels can be substituted. This reconstruction closes the loop: idle periods collapse into long IBGs, bursts are preserved with their predicted magnitudes, and the output recovers a time series that retains the statistical properties of the original telemetry time series and can be used by downstream task that require forecasting.

## 4 EVALUATION

We evaluate NETBURST on both canonical forecasting benchmarks and production network telemetry time series. Our goal is to test whether an event-centric design improves forecasting fidelity under bursty, heavy-tailed conditions, and whether the learned representations carry semantic information useful for downstream tasks. This section describes datasets, baselines, experimental protocols, evaluation metrics, and results.

### 4.1 EXPERIMENTAL SETUP

**Datasets and preprocessing.** We evaluate NETBURST on both standard time-series forecasting benchmarks and large-scale networking telemetry datasets. The benchmarks include the earlier-mentioned Electricity, Taxi, ETT, Exchange Rate, and Weather datasets, each preprocessed at their originally reported sampling resolutions. For network telemetry, we use two major sources: PINOT and MAWI. Specifically, the PINOT dataset contains packet traces (1.98 billion packets) collected from a campus gateway router for the week of Dec 10th 2023 over 13 15-minute intervals, while the MAWI dataset contains packet traces (23 million packets) collected from an ISP backbone router on 24th May 2025, over a single 15-minutes interval. From these traces, we generate time series repre-

Dataset	Service	IP	Subnet
PINOT (100 ms)	20.5M	1.81M	737K
PINOT (1 s)	7.44M	931k	361K
MAWI (100 ms)	1.35M	753K	157K
MAWI (1 s)	1.08M	743K	135K

Table 2: Number of time series in telemetry datasets.

senting the number of bytes transferred, aggregating packets at different temporal granularities (from milliseconds to minutes) and spatial levels (service, IP, and /24 subnet). Unless otherwise specified, we report results at 100 ms resolution for service time series and 1 s IP and subnet time series. These intervals are both operationally relevant (service level classification and quality estimation tasks require faster decision-making compared to IP- or subnet-level aggregation for anomaly detection or traffic engineering tasks). As shown in Figure 3, they strike a balance in capturing traffic dynamics: smaller windows expose fine-grained bursts but increase sparsity, whereas larger windows suppress variability and obscure burst structure. Table 2 summarizes the number of time series at service, IP, and subnet granularities at these two temporal resolutions.

**Baselines.** We compare NETBURST against both foundation-style and classical forecasters to ensure coverage of the most competitive and representative approaches. Chronos-T5 (Ansari et al., 2024) is included as a strong foundation baseline: it uses uniform binning and large-scale pre-training, making it the most direct point of comparison for our quantile-based tokenization. Lag-Llama (Rasul et al., 2023b) represents recent autoregressive foundation models that emphasize cross-dataset transfer, allowing us to test whether broad pretraining and simple AR decoding suffice for bursty, event-driven telemetry data. DeepAR (Salinas et al., 2020) provides a probabilistic RNN baseline with likelihood-based training, probing whether explicit probabilistic modeling captures tails and uncertainty relevant to rare-event forecasting. Finally, N-BEATS (Oreshkin et al., 2020) serves as a strong non-attention baseline with trend/seasonality inductive biases, testing whether generic deep residual architectures perform adequately on data with weak global seasonality but heavy-tailed local burst structure.

All baselines are tuned with comparable hyperparameter budgets to ensure fairness in evaluation. Table 3 summarizes all hyperparameters. We use early stopping with a patience of 10 validation evaluations (monitoring validation loss) and select the best checkpoint. For a fair comparison, we fix the context length and batch size across all models; other settings follow each baseline’s recommended configuration unless noted otherwise.

Table 3: Baseline hyperparameters (paper-aligned recommendations). Where papers specify ranges or dataset-dependent choices, we list the range/guideline rather than a single value.

Baseline	Context length	Batch size	Hidden size	Vocabulary	Learning rate	Optimizer
DeepAR	512	32	64	—	$\sim 1 \times 10^{-4}$	Adam
N-BEATS	512	32	512	—	$\sim 1 \times 10^{-3}$	Adam
Chronos-T5	512	32	512	4096 bins	$\sim 1 \times 10^{-3}$	Adam
Lag-Llama	512	32	144	—	$\sim 1 \times 10^{-4}$	Adam
NetBurst	512	32	512	4096 bins	$\sim 1 \times 10^{-4}$	Adam

**Training protocols and implementation.** To ensure fairness, all models follow identical protocols. Time series are split chronologically into 70% training/context, 20% testing, and 10% validation. Eventization is applied post-split: IBG and BI sequences are recomputed for each  $T_{\text{act}}$ , with quantile codebooks fit only on training data to prevent leakage. At inference, IBG and BI heads decode autoregressively, and predictions are mapped via codebook centroids. Metrics are averaged across entities and reported by granularity and threshold. We use Adam (Kingma & Ba, 2014) with learning rate  $1 \times 10^{-4}$ , batch size 32, and early stopping on validation loss. NETBURST uses a 12-layer seq2seq transformer (hidden size 512), following Chronos but replacing uniform bins with 4096-bin quantile codebooks to preserve both small fluctuations and large bursts. All baselines use the same optimizer, batch size, and early stopping policy. A detailed account of all hyperparameters used for the different baselines and their values is provided in Table 3.

**Evaluation metrics.** We compute Absolute Scaled Error (ASE) to capture pointwise accuracy relative to ground truth. We report both the mean of ASE (MASE) and its full distribution across entities and horizons, which reveals where errors concentrate and highlights rare but operationally critical failures. To mitigate sparsity bias, we compute MASE only on events, following prior work (Zuo et al., 2020; Meng et al., 2024). Finally, we use the 1-Wasserstein Distance (WD) to assess distributional fidelity by jointly evaluating burst timing and magnitude.

## 4.2 NETBURST VS. BASELINES

### Does NETBURST offer significant gains on bursty and intermittent network telemetry data?

We begin with the most challenging regime: service-level time series at 100 ms resolution. Figure 4 highlights forecasting performance for both PINOT and MAWI. On PINOT service data, NETBURST achieves a MASE of 0.0766, while the strongest baseline (DeepAR) records 1.00—a  $13\times$  higher MASE. Lag-Llama fares worse at 2.29 ( $30\times$  higher), and Chronos-T5 and N-BEATS collapse catastrophically at 18.1 ( $237\times$ ) and 46.3 ( $605\times$ ) respectively. A similar pattern holds for MAWI service traces, where NETBURST reaches 0.0762 versus DeepAR’s 1.00 ( $13\times$  higher) and Lag-Llama’s 1.02 ( $13.3\times$  higher), with Chronos-T5 at 2.18 ( $28.6\times$ ) and N-BEATS at 35.6 ( $467\times$ ).

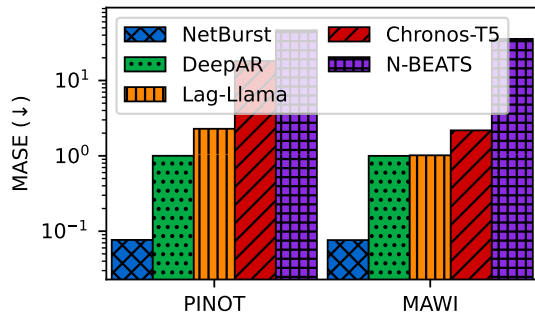


Figure 4: NETBURST vs. Baselines

Table 4: Relative MASE for existing SOTA forecasters versus NETBURST (smaller is better). Each entry shows how much worse the baseline error is compared to NETBURST (first column) on the same telemetry dataset.

Dataset	NETBURST (MASE)	DeepAR	Lag-Llama	Chronos	N-BEATS
PINOT-service	0.0766	13.1×	29.8×	236.8×	605.1×
PINOT-IP	0.8963	2.46×	2.92×	872.8×	96.5×
PINOT-subnet	0.9553	2.07×	2.07×	1717.2×	100.0×
MAWI-service	0.0762	13.1×	13.3×	28.6×	466.6×
MAWI-IP	7.1546	1.23×	4.83×	227.8×	6.28×
MAWI-subnet	4.3533	1.18×	3.17×	3.09×	22.7×

These results confirm our central hypothesis: NETBURST delivers order-of-magnitude gains in the most bursty and intermittent settings, where prior SOTA models fail.

Table 4 shows this comparison across all granularities. On PINOT IP-level data, NETBURST reduces error to 0.90, compared to 2.20 (2.5× higher) for DeepAR and 2.62 (2.9×) for Lag-Llama. On PINOT subnet data, NETBURST achieves 0.96, again halving the error relative to DeepAR and Lag-Llama (both at  $\sim 2.0$ ). For MAWI, NETBURST records 7.15 MASE at the IP level versus 8.83 (1.2× higher) for DeepAR and 34.5 (4.8×) for Lag-Llama. At the subnet level, NETBURST attains 4.35 compared to 5.13 (1.2×) for DeepAR and 13.8 (3.2×) for Lag-Llama. While the margins are smaller at coarser granularities—reflecting the reduced sparsity of aggregated flows—NETBURST consistently outperforms baselines. Importantly, models like Chronos-T5 and N-BEATS collapse in nearly every case, producing errors that are two to three orders of magnitude larger than NETBURST.

An examination of the error distributions further illustrates this gap. Figure 5 plots the CDF of absolute scaled errors for PINOT across all granularities (linear scale, excluding the worst baselines Chronos and N-BEATS). NETBURST shifts the error mass consistently leftward compared to both DeepAR and Lag-Llama, yielding tighter and lower error distributions. A notable pathology emerges: DeepAR collapses in sparse regimes by learning a “always zero” forecast. While this forecast reduces error superficially on quiescent intervals, it fails catastrophically on bursts, exposing a vulnerability of sequence models to shortcut learning in sparse domains. NETBURST, by contrast, maintains robustness across both sparse and dense regions.

**Does NETBURST preserve burstiness while decomposing forecasts?** A critical concern is whether decomposing traffic into inter-burst gaps and burst intensities compromises burstiness in the reconstructed series. We address this by reporting in Table 5 the Wasserstein distance (WD), which evaluates distributional fidelity. On the most challenging service-level time series, NETBURST achieves WD values of 0.0006 (PINOT) and 0.0009 (MAWI), which are comparable to DeepAR (0.0006 / 0.0001) and Lag-Llama (0.0005 / 0.0002). These results demonstrate that the large MASE gains of NETBURST on bursty intermittent data do not come at the expense of distorted distributional structure. At coarser granularities, NETBURST in fact improves WD relative to strong baselines: on PINOT subnet data, it attains 0.0067, outperforming Lag-Llama (0.0101) and DeepAR (0.0105), and on MAWI subnet, it reaches 0.0112, improving on Lag-Llama (0.0332) and DeepAR (0.0254). Taken together, these results show that NETBURST’s event-centric decomposi-

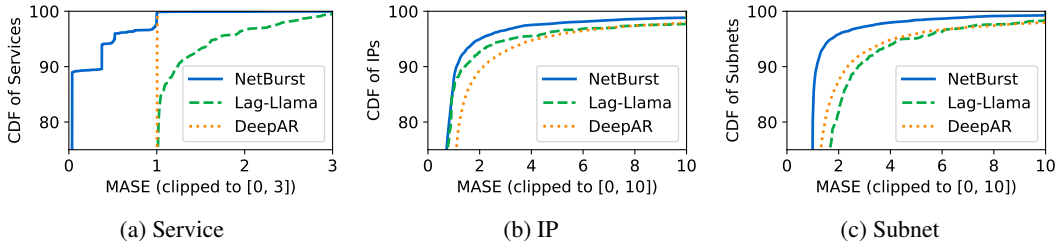


Figure 5: CDF of MASE losses shows NETBURST has fewer examples where losses were large, demonstrating effectiveness in predicting rare events.

tion preserves or enhances burstiness fidelity across all granularities, while delivering substantial pointwise error reductions where they matter most.

Table 5: Wasserstein distance (WD; ↓ lower is better) on networking datasets (100 ms and 1 s).

Dataset	NETBURST	DeepAR	Lag-Llama	N-BEATS	Chronos-T5
PINOT-service	0.0006	0.0006	0.0005	0.0193	0.0020
PINOT-IP	0.0069	0.0080	0.0071	0.0220	0.4174
PINOT-subnet	0.0067	0.0105	0.0101	0.0376	1.0639
MAWI-service	0.0009	0.0001	0.0002	0.0042	0.0010
MAWI-IP	0.0253	0.0352	0.0484	0.0361	2.5553
MAWI-subnet	0.0112	0.0254	0.0332	0.1439	0.0272

### 4.3 ABLATION STUDIES

**Do quantile codebooks improve fidelity over uniform binning?** A central design choice in NETBURST is to replace uniform binning, as employed by Chronos, with distribution-aware quantile-based tokenization. Quantile codebooks allocate resolution according to probability mass, ensuring that rare, high-magnitude bursts are well represented, while uniform binning wastes tokens on dense regions and undersamples the tails. To isolate this effect, we evaluate three models at each granularity (service, IP, subnet): (i) Chronos as-is (i.e., using uniform binning), (ii) a variant of Chronos that replaces uniform bins with quantile-based codebooks while keeping the rest of the architecture unchanged, and (iii) NETBURST, which combines quantile-based tokenization with stream decomposition via dual models.

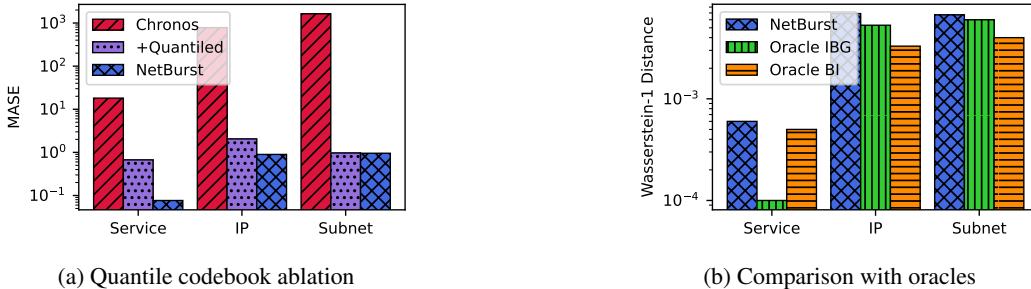


Figure 6: Ablation study.

Figures 6a show that moving from uniform to quantile binning consistently lowers MASE and WD (not shown for brevity), with the largest gains on service traces where burstiness is most severe. Notably, the performance gap between models (ii) and (iii) diminishes at coarser granularities, indicating that quantile-based tokenization contributes the bulk of the improvement for IP and subnet. In contrast, at the finer and more bursty service level, the full combination of quantile binning and stream decomposition is most effective. These results confirm that quantile-based tokenization is not an incidental detail but a critical design choice, while disentangling streams adds further leverage in the most challenging sparse regimes.

**Where does residual error come from: timing or magnitude?** Finally, we ask whether residual error is primarily due to imperfect modeling of inter-burst timing or burst magnitudes. To answer this, we evaluate three variants: (i) the trained NETBURST model, (ii) Oracle-IBG, which substitutes ground-truth inter-burst gaps while keeping predicted burst intensities, and (iii) Oracle-BI, which substitutes ground-truth burst intensities while keeping predicted inter-burst gaps. Figure 6b shows that on IP and subnet data, Oracle-BI reduces WD more than Oracle-IBG, implicating magnitude alignment as the dominant residual source. On service traces, however, Oracle-IBG closes more of the gap, indicating that timing dominates in the sparsest regime. These results suggest that future improvements should target stronger temporal modeling for service, while magnitude modeling is the higher-leverage direction for coarser granularities.

#### 4.4 MODEL TRANSFERABILITY

**Hypothesis.** The bursty and intermittent temporal dynamics of network telemetry time series, often referred to as the fractal or self-similar nature of network traffic (Willinger et al., 2002), enables effective cross-granularity transfer: a model pre-trained at a finer granularity (e.g., service-level traces) can be adapted to coarser granularities (e.g., IP, subnet) by thresholding small values as noise, thereby aligning their statistical structure. If true, this would allow operators to reuse a single pre-trained model across granularities with minimal fine-tuning, avoiding the cost of per-granularity pre-training.

**Does thresholding reveal distributional similarity across granularities?** Sparsity in network telemetry time series allows for a natural partitioning into "interesting" (nontrivial activity) and "uninteresting" (idle or negligible activity) windows. Crucially, what counts as interesting depends on the aggregation granularity. By thresholding activity, quantizing active windows with global quantile binning, and measuring entropy, we find that once low-activity windows are suppressed, the statistical structure self-repeats across levels. Figure 7a reports the Jensen-Shannon divergence (JSD) between service-level traces and thresholded IP/subnet-level traces. As the threshold  $T_{act}$  increases (100, 200, 300 bytes), the JSD decreases monotonically, indicating that thresholding progressively aligns coarser time series distributions with service-level distributions. This fractal behavior reaffirms the self-similarity of network traffic, extensively studied in prior work such as (Willinger et al., 2002; Leland et al., 2002; Taqqu et al., 1997), and highlights its modern implications for learning: models can, in principle, transfer across granularities.

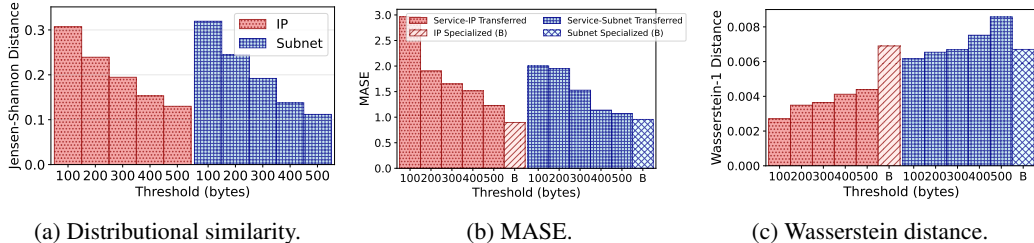


Figure 7: MASE and WD of service model when adapted to tokenizers based on IP and subnet datasets under different thresholds.

**Does a service-level pretrained model transfer effectively to coarser granularities?** We next test whether this statistical similarity translates into model performance. Figures 7b and 7c show MASE and WD, respectively, for service-pretrained models transferred to IP and subnet datasets under different thresholds, compared against specialized IP/subnet-pretrained references. Two consistent trends emerge. First, as  $T_{act}$  increases, MASE decreases because small fluctuations are ignored and the forecast focuses on salient bursts. Second, WD increases slightly because thresholding shifts mass into zeros and introduces residual timing or magnitude mismatches on micro-activity. Importantly, at higher thresholds (200–300 bytes), the transferred service-pretrained model nearly matches the specialized models on both MASE and WD. This demonstrates the feasibility of cross-granularity transfer: one NETBURST model pre-trained on fine-grained service data can generalize to coarser granularities with minimal fine-tuning.

**Implications.** In practice, these findings offer significant efficiency advantages. Network operators may aggregate traffic differently across settings, and retraining per-granularity models would be costly. By leveraging the fractal or self-similarity nature of network telemetry time series and applying thresholding transformations, NETBURST can be pre-trained once at fine granularity and adapted across granularities, preserving fidelity while reducing training costs. This supports the broader vision of NETBURST as a foundation model for network telemetry time series that generalizes across both temporal and spatial scales.

#### 4.5 REPRESENTATIONAL QUALITY OF EMBEDDINGS

Beyond forecasting accuracy, it is critical to assess whether NETBURST’s event-centric embeddings provide richer representational quality than baseline models. To this end, we use a mix of volumetric traces from the PINOT dataset. These traces serve as “cross-traffic profiles” (CTPs) that enable emulating realistic network dynamics in controlled settings (Daneshamooz et al., 2025). Clustering CTPs with similar causal effects on network applications competing for limited resources at a bottleneck link is essential for scaling meaningful data generation in such emulators. We therefore evaluate the quality of NETBURST embeddings by studying their ability to group 50k CTPs subsampled from PINOT’s campus network traces.

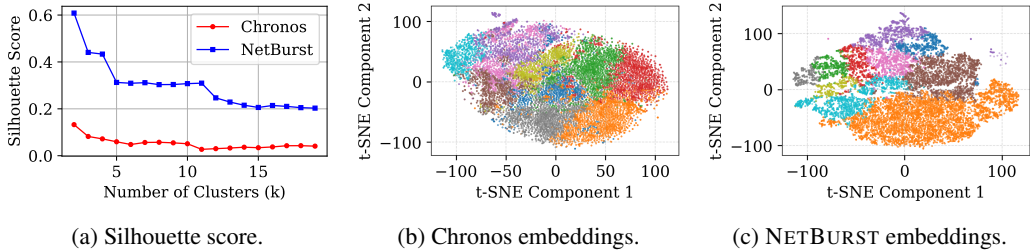


Figure 8: Representational quality of embeddings extracted from IP-level traces. NETBURST reduces anisotropy and improves clustering, yielding semantically richer embeddings.

We apply  $k$ -means clustering on the embeddings and measure the silhouette score as  $k$  varies. Higher silhouette scores indicate clearer grouping of similar time series, while lower scores suggest overlapping or poorly separated clusters. Figure 8(a) shows that Chronos embeddings yield consistently low silhouette scores across all  $k$ , whereas NETBURST embeddings achieve substantially higher values, improving by more than  $5\times$  at small  $k$ . To qualitatively assess this effect, we project embeddings into two dimensions using t-SNE. Figures 8(b) and 8(c) illustrate the clustering behavior of Chronos and NETBURST. Chronos embeddings collapse into overlapping regions with weak separation, consistent with their higher anisotropy and low silhouette scores. In contrast, NETBURST embeddings form distinct, well-structured groups that align with different CTP behaviors, reflecting stronger clustering capability. Taken together, these results show that NETBURST not only improves forecasting accuracy but also produces semantically richer embeddings that transfer more effectively to downstream grouping and classification tasks.

## 5 DISCUSSION: BROADER IMPACT AND LIMITATIONS

**Model transferability.** Our transferability analysis in Section 4.4 builds on the hypothesis that the bursty, self-similar nature of network telemetry data allows statistical structure to repeat across granularities. Specifically, once small fluctuations are suppressed, time series at coarser levels (IP, subnet) begin to resemble their fine-grained counterparts (service), enabling cross-granularity reuse. Empirically, we find that service-pretrained models can be adapted to IP and subnet series by thresholding low-activity windows: distributional similarity improves monotonically with higher thresholds, and the transferred model nearly matches the performance of specialized per-level models on both MASE and WD. These results provide the first concrete evidence that a single event-centric model, trained at fine granularity, can generalize across spatial scales with minimal fine-tuning. Beyond cost savings, this supports the broader vision of NETBURST as a foundation model for telemetry—one capable of leveraging fractal-like scaling to unify forecasting across heterogeneous

---

granularities and operational settings. Realizing this promise more fully, especially for other self-similar time series beyond networking, remains an exciting direction for future work.

**Operational practice.** Accurate burst forecasting directly supports operators in congestion anticipation, anomaly detection, and capacity planning. Event-centric embeddings also provide transferable representations for downstream tasks such as traffic classification and policy-driven control. More broadly, viewing forecasting as representation learning creates opportunities for transfer across datasets and domains.

**Beyond networking.** The statistical regime we target—bursty, intermittent, heavy-tailed time series—extends well beyond networking. Financial transactions, reliability logs, epidemic outbreaks, and climate extremes all exhibit irregular bursts separated by long idle periods. By decoupling timing from magnitude, NETBURST offers a general event-centric paradigm for forecasting processes where rare, high-impact events matter more than averages.

**Limitations of our approach& outlook.** NETBURST currently models bursts as spikes with aggregated intensity, ignoring intra-burst structure; richer kernels or learned profiles could capture within-burst dynamics. Eventization relies on fixed thresholds, whereas adaptive or learned thresholds may yield more flexible decompositions. Finally, residual errors are dominated by timing (Oracle-IBG), motivating exploration of hierarchical Hawkes-like models or uncertainty-aware predictors.

## 6 CONCLUSION

On large-scale telemetry datasets (PINOT, MAWI), NETBURST reduces MASE by 13–605× compared to state-of-the-art forecasters at the bursty and intermittent service-level granularity, while consistently preserving burstiness across all levels, achieving up to 3× better Wasserstein distance at the subnet level. These gains, concentrated on rare, high-intensity bursts, stem from NETBURST’s event-centric design: reframing forecasting as predicting *when* bursts occur and *how large* they are, using quantile-based codebooks and dual autoregressors. By allocating capacity to extreme events while retaining distributional fidelity, NETBURST overcomes the limitations of transformer forecasters and point-process models that smooth away or collapse under heavy tails. This work establishes forecasting of bursty, intermittent, heavy-tailed time series—long recognized in Mandelbrot’s work on self-similar scaling phenomena—as both an operationally critical and scientifically under-explored challenge, and positions NETBURST as a step toward foundation models that learn the language of rare extremes across networking, finance, climate, and beyond.

## REPRODUCIBILITY STATEMENT

We have made every effort to ensure that our work is reproducible. An anonymized repository accompanies this submission and includes: (i) pointers to the raw, publicly accessible MAWI dataset used in our experiments (noting that raw PINOT data is not publicly available); (ii) pointers to fully anonymized, pre-processed datasets used for analysis; and (iii) pre-processing scripts, model training code, and experiment configurations corresponding to the evaluations reported in Section 4. The anonymized repository for NetBurst can be found at <https://anonymous.4open.science/r/NetBurst-F135/>. Together with the methodological details provided in the paper, these resources are intended to facilitate faithful reproduction of our results.

## ETHICS STATEMENT

All authors have read and adhered to the ICLR Code of Ethics. This research does not involve human subjects directly. However, packet traces may contain personally identifiable information (PII), which raises privacy considerations. We have therefore taken extensive measures to ensure responsible data handling and compliance with institutional and ethical standards.

Our data collection and research protocols were reviewed and exempted by the university’s Institutional Review Board (IRB). Because the dataset originates from an operational campus network, the collection and research processes were also reviewed by a separate institutional committee comprising campus stakeholders and IT experts, which approved the use of this dataset for research

---

purposes. All researchers accessing the dataset completed mandatory training in research ethics and data privacy.

**Anonymization.** To minimize privacy risks, we only collect a minimal subset of packet header fields. Packet payloads are discarded beyond RTP header extensions. Internal (campus) IP addresses are anonymized in a prefix-preserving manner at the building level using a modified ONTAS system (Kim & Gupta, 2019), implemented directly in the hardware switch via P4. This ensures that traffic is anonymized *before* reaching the collection server. External (non-campus) IP addresses are preserved to enable analysis of Autonomous Systems and application-level behavior (e.g., Zoom). While such addresses could theoretically be linked to users, they are typically associated with large ISPs or enterprises and are dynamically assigned, making re-identification infeasible. No effort was made to deanonymize or identify any individual user.

**Data management.** The campus dataset is stored in a secure infrastructure managed by professional IT staff. Access is strictly limited to IRB-approved researchers and authorized IT personnel. The dataset cannot be moved or copied outside the secure environment, ensuring compliance with institutional data protection requirements.

We believe these safeguards adequately address potential ethical concerns regarding privacy, security, and responsible research conduct.

## ACKNOWLEDGEMENT

The authors thank Dr. Chris Misa (University of Oregon) for thoughtful feedback on our problem formulation and experiments. This work was supported in part by the National Science Foundation (CAREER Award No. 2443777 and CNS Award No. 2323229) and a research gift from Cisco. This research used resources of the National Energy Research Scientific Computing Center, a DOE Office of Science User Facility supported by the Office of Science of the U.S. Department of Energy under Contract No. DE-AC02-05CH11231 using NERSC award NERSC DDR-ERCAP0029768. We gratefully acknowledge access to NERSC GPU systems that enabled the large-scale training and evaluation in this work.

## REFERENCES

- Wide mawi working group. <https://mawi.wide.ad.jp/>, 2025. Network traffic measurement and analysis from the WIDE Project.
- Abdul Fatir Ansari, Lorenzo Stella, Caner Türkmen, Xiyuan Zhang, Pedro Mercado, Huibin Shen, Oleksandr Shchur, Syama Syndar Rangapuram, Sebastian Pineda Arango, Shubham Kapoor, Jasper Zschiegner, Danielle C. Maddix, Michael W. Mahoney, Kari Torkkola, Andrew Gordon Wilson, Michael Bohlke-Schneider, and Yuyang Wang. Chronos: Learning the language of time series. *Transactions on Machine Learning Research*, 2024. ISSN 2835-8856. URL <https://openreview.net/forum?id=gerNCVqqtR>.
- Roman Beltiukov, Sanjay Chandrasekaran, Arpit Gupta, and Walter Willinger. Pinot: Programmable infrastructure for networking. In *Proceedings of the 2023 Applied Networking Research Workshop*, pp. 51–53, 2023.
- Jan Beran. Statistics for long-memory processes. 1994. URL <https://api.semanticscholar.org/CorpusID:62495143>.
- George EP Box, Steven C Hillmer, and George C Tiao. Analysis and modeling of seasonal time series. In *Seasonal analysis of economic time series*, pp. 309–344. NBER, 1978.
- George EP Box, Gwilym M Jenkins, Gregory C Reinsel, and Greta M Ljung. *Time series analysis: forecasting and control*. John Wiley & Sons, 2015.
- Jaber Daneshamooz, Jessica Nguyen, William Chen, Sanjay Chandrasekaran, Satyandra Guthula, Ankit Gupta, Arpit Gupta, and Walter Willinger. Addressing the ml domain adaptation problem for networking: Realistic and controllable training data generation with netreplica. *arXiv preprint arXiv:2507.13476*, 2025.

- 
- Ugo Fano. Ionization yield of radiations. ii. the fluctuations of the number of ions. *Physical Review*, 72(1):26, 1947.
- Federal Reserve. Exchange rates. Kaggle Datasets, 2022. <https://www.kaggle.com/datasets/federalreserve/exchange-rates>.
- Chin Guok, Ed Balas, Sowmya Balasubramanian, Justas Balcas, Jaber Daneshamooz, Sukhada Gholba, Mike Haberman, Shawn Kwang, John MacAuley, Sam Moats, and others. ES-net Data and AI Workshop Report. Technical report, Lawrence Berkeley National Laboratory (LBNL), Berkeley, CA (United States), June 2025. URL <https://www.osti.gov/biblio/2571672>.
- Ali Hasan, Yuting Ng, Jose Blanchet, and Vahid Tarokh. Representation learning for extremes. In *NeurIPS 2023 Workshop Heavy Tails in Machine Learning*, 2023.
- Alan G Hawkes. Spectra of some self-exciting and mutually exciting point processes. *Biometrika*, 58(1):83–90, 1971.
- Hyoon Kim and Arpit Gupta. Ontas: Flexible and scalable online network traffic anonymization system. In *Proceedings of the 2019 Workshop on Network Meets AI & ML, NetAI'19*, pp. 15–21, New York, NY, USA, 2019. Association for Computing Machinery. ISBN 9781450368728. doi: 10.1145/3341216.3342208. URL <https://doi.org/10.1145/3341216.3342208>.
- Diederik P. Kingma and Jimmy Ba. Adam: A method for stochastic optimization. *CoRR*, abs/1412.6980, 2014. URL <https://api.semanticscholar.org/CorpusID:6628106>.
- Will E Leland, Murad S Taqqu, Walter Willinger, and Daniel V Wilson. On the self-similar nature of ethernet traffic (extended version). *IEEE/ACM Transactions on networking*, 2(1):1–15, 2002.
- Bryan Lim and Stefan Zohren. Time-series forecasting with deep learning: a survey. *Philosophical Transactions of the Royal Society A*, 379(2194):20200209, 2021.
- Benoit B. Mandelbrot. *The Fractal Geometry of Nature*. W. H. Freeman, New York, 1982.
- Benoit B. Mandelbrot. *Fractals and Scaling in Finance: Dicontinuity, Concentration, Risk*. Springer, 1997.
- David M. Mason. The hurst phenomenon and the rescaled range statistic. *Stochastic Processes and their Applications*, 126(12):3790–3807, 2016. ISSN 0304-4149. doi: <https://doi.org/10.1016/j.spa.2016.04.008>. URL <https://www.sciencedirect.com/science/article/pii/S0304414916300308>. In Memoriam: Evarist Giné.
- Zizhuo Meng, Ke Wan, Yadong Huang, Zhidong Li, Yang Wang, and Feng Zhou. Interpretable transformer hawkes processes: Unveiling complex interactions in social networks. In *Proceedings of the 30th ACM SIGKDD Conference on Knowledge Discovery and Data Mining, KDD '24*, pp. 2200–2211, New York, NY, USA, 2024. Association for Computing Machinery. ISBN 9798400704901. doi: 10.1145/3637528.3671720. URL <https://doi.org/10.1145/3637528.3671720>.
- Shubham Misar. Nyc-taxi — time series — lstm. Kaggle Code, 2022. <https://www.kaggle.com/code/shubhammisar/nyc-taxi-time-series-lstm>.
- Jayakrishnan Nair, Adam Wierman, and Bert Zwart. The fundamentals of heavy-tails: properties, emergence, and identification. In *Measurement and Modeling of Computer Systems*, 2013. URL <https://api.semanticscholar.org/CorpusID:207203374>.
- Boris N. Oreshkin, Dmitri Carпов, Nicolas Chapados, and Yoshua Bengio. N-BEATS: Neural basis expansion analysis for interpretable time series forecasting. In *International Conference on Learning Representations*, 2020. URL <https://openreview.net/forum?id=rlecqn4YwB>.
- Victor M Panaretos and Yoav Zemel. Statistical aspects of wasserstein distances. *Annual review of statistics and its application*, 6(1):405–431, 2019.

- 
- Kashif Rasul, Arjun Ashok, Andrew Robert Williams, Arian Khorasani, George Adamopoulos, Rishika Bhagwatkar, Marin Biloš, Hena Ghonia, Nadhir Hassen, Anderson Schneider, et al. Lag-llama: Towards foundation models for time series forecasting. In *R0-FoMo: Robustness of Few-shot and Zero-shot Learning in Large Foundation Models*, 2023a.
- Kashif Rasul, Arjun Ashok, Andrew Robert Williams, Arian Khorasani, George Adamopoulos, Rishika Bhagwatkar, Marin Biloš, Hena Ghonia, Nadhir Hassen, Anderson Schneider, Sahil Garg, Alexandre Drouin, Nicolas Chapados, Yuriy Nevmyvaka, and Irina Rish. Lag-Llama: Towards Foundation Models for Time Series Forecasting. In *R0-FoMo Workshop at NeurIPS 2023*, 2023b. URL <https://openreview.net/forum?id=jYluzCLFDM>.
- Sidney I. Resnick. *Heavy-Tail Phenomena: Probabilistic and Statistical Modeling*. Springer New York, 2007.
- David Salinas, Valentin Flunkert, Jan Gasthaus, and Tim Januschowski. DeepAR: Probabilistic forecasting with autoregressive recurrent networks. *International Journal of Forecasting*, 2020. ISSN 0169-2070. doi: <https://doi.org/10.1016/j.ijforecast.2019.07.001>. URL <https://www.sciencedirect.com/science/article/pii/S0169207019301888>.
- Ketan Rajshekhar Shahapure and Charles Nicholas. Cluster quality analysis using silhouette score. In *2020 IEEE 7th international conference on data science and advanced analytics (DSAA)*, pp. 747–748. IEEE, 2020.
- Murad S Taqqu, Walter Willinger, and Robert Sherman. Proof of a fundamental result in self-similar traffic modeling. *ACM SIGCOMM Computer Communication Review*, 27(2):5–23, 1997.
- Artur Trindade. ElectricityLoadDiagrams20112014. UCI Machine Learning Repository, 2015. DOI: <https://doi.org/10.24432/C58C86>.
- Victor Verma, Stilian Stoev, and Yang Chen. On the optimal prediction of extreme events in heavy-tailed time series with applications to solar flare forecasting, 2025. URL <https://arxiv.org/abs/2407.11887>.
- Adam Wierman. An introduction to heavy tails for ml researchers. Keynote at NeurIPS 2023 Workshop on Heavy Tails in Machine Learning, 2023. URL [https://www.di.ens.fr/~simsekli/ht\\_ml\\_2023/wierman.pdf](https://www.di.ens.fr/~simsekli/ht_ml_2023/wierman.pdf).
- Walter Willinger, Murad S Taqqu, Robert Sherman, and Daniel V Wilson. Self-similarity through high-variability: statistical analysis of ethernet lan traffic at the source level. *IEEE/ACM Transactions on networking*, 5(1):71–86, 2002.
- Walter Willinger, David Alderson, John Doyle, and Lun Li. More "normal" than normal: Scaling distributions and complex systems. volume 1, pp. – 141, 01 2005. ISBN 0-7803-8786-4. doi: 10.1109/WSC.2004.1371310.
- Haoyi Zhou, Shanghang Zhang, Jieqi Peng, Shuai Zhang, Jianxin Li, Hui Xiong, and Wancai Zhang. Informer: Beyond efficient transformer for long sequence time-series forecasting. In *Proceedings of the AAAI conference on artificial intelligence*, volume 35, pp. 11106–11115, 2021.
- Simiao Zuo, Haoming Jiang, Zichong Li, Tuo Zhao, and Hongyuan Zha. Transformer Hawkes process. In Hal Daumé III and Aarti Singh (eds.), *Proceedings of the 37th International Conference on Machine Learning*, volume 119 of *Proceedings of Machine Learning Research*, pp. 11692–11702. PMLR, 13–18 Jul 2020. URL <https://proceedings.mlr.press/v119/zuo20a.html>.